Int. J. Multiphase Flow Vol. 16, No. 1, pp. 91–102, 1990
Printed in Great Britain.

0301-9322/90 $3.00 + 0.00

EFFECTS OF CHARGES ON THE PARTICLE MOTION ABOVE FLUIDIZED BEDS

H. RASZILLIER, F. DURST and B. MOHR
Lehrstuhl für Strömungsmechanik, Universität Erlangen-Nürnberg, Egerlandstr. 13, 8520 Erlangen, B.R.D.

(*Received* 19 *October* 1988; *in revised form* 13 *June* 1989)

Abstract—The paper is concerned with the effects of electric charges on the motion of metallically coated particles in fluidized beds. It treats a particular kind of collision process between such particles, which happens on the upper layers of such a bed. Photographic studies are provided displaying the phenomenon. In order to explain it, the interaction of a pair of spherical charged particles surrounded by a dielectric fluid is analyzed theoretically. It is shown that the peculiarities of the collision are related to the fact that two conducting particles of the same diameter, even if they have charges of the same sign, but of different magnitude, attract each other when they approach close enough and that they repel after collision because of the charge redistribution between them. It turns out that the experimental observations are well-described by this theoretical picture.

Key Words: fluidized bed, particle collision, electric charge

1. INTRODUCTION

This paper concerns particle motion caused by electric charges, observed by the authors during velocity measurements in a homogeneous fluidized bed. When such beds were produced by dielectric fluids, particle motions on top of the bed, controlled by electrostatic rather than by fluid dynamic and/or gravity forces, were observed.

The phenomenon appeared as follows. In order to get accurate results of velocity distributions of the fluid in the inner part of the fluidized bed by optical methods (LDA), a refractive index adjustment of the fluid and particles (glass spheres of diameter $D = 0.315$ cm) had to be performed. The adjustment eliminated the spheres optically and made the entire bed transparent; the glass particles became invisible. In order to get information on the motion of the particles, a small sample of them had been covered by a thin metallic sheet to make them visible.

It was intended to keep these few nontransparent particles in their fluid dynamic and gravitational behaviour very close to the uncoated spheres. It turned out, however, that the coated particles developed a behaviour of their own. Most of them moved out of the bed and gathered in a layer above it. Sometimes, they reached heights up to 5 to 10 cm and then fell down close to the bed. There seemed to be a mechanism present, which kept the metallic particles, to a large extent, above the bed and concentrated them near the pipe axis.

A remarkable motion was observed when a metallically coated sphere settled down due to gravity and hit another such sphere floating above the fluidized bed: when the settling particle approached close enough to the lower one (a few mm) it was strongly accelerated towards it; after contact it was shot rapidly back upwards. This phenomenon can hardly be described by inertial, friction, or gravitational effects, but rather naturally as one caused by electric charges.

In the paper the experimental observations are described and it is shown that they can be explained in terms of electrostatic forces between electrically charged conducting spheres. The question of the origin of the charges—most likely tribologic—is not pursued.

The reason for the relevance of electrostatic forces between two spheres appears as follows. If one assumes that two (identical) spheres carry charges Q_1 and Q_2, then the forces between them have the following characteristics:

- $Q_1 Q_2 < 0$. There is always an attractive force between the charges, essentially of Coulomb type.

- $Q_1 = 0, Q_2 \neq 0$. In this case, particles of finite size develop an attractive force between the charge Q_2 and the charge distribution induced on the other sphere. This force is significant only when the surface distance of the spheres come down to the order of magnitude of the sphere size (radius); only then is the induced charge distribution significant.
- $Q_1 Q_2 > 0, Q_1 \neq Q_2$. Charges of the same sign, but unequal magnitude develop a (dominantly Coulomb) repulsion between the spheres at large distances. At small enough distances the bigger charge induces on the other sphere a charge density of opposite sign, which may come to dominate the (Coulomb) repulsion. There is a certain limiting distance, depending on the ratio $[(Q_1 - Q_2)/(Q_1 + Q_2)]^2$, such that above it the two spheres repel, whereas below it they attract each other.
- $Q_1 = Q_2$. For equal charges two identical spheres are subject at all distances to repulsive electric forces.

With these characteristics of charged spheres in mind, one may imagine the following situation. Two conducting spheres, one settling from some distance above the fluidized bed and the other settled just on top of it, carry the charges $Q_1^i = 0, Q_2^i > 0$, respectively. The settling upper sphere will first perceive only the usual gravity and viscosity forces leading to a rather constant settling velocity. At a short distance from the lower sphere the attractive electric force accelerates it until the two spheres come into contact. While in contact, the particles redistribute their charges $Q_1^i \rightarrow Q_1^f, Q_2^i \rightarrow Q_2^f, Q_1^f = Q_2^f, Q_1^f + Q_2^f = Q_1^i + Q_2^i$. Charge equality between them then leads to a repulsive electric force. If the charges $Q_1^f = Q_2^f$ are big enough, the formerly settling sphere will be strongly accelerated upwards, the other downwards. This acceleration of the upper sphere lasts until the repulsive Coulomb force becomes smaller than that of gravity.

The observed phenomenon is described in section 2. The theoretical explanation is presented in sections 3 and 4, followed by remarks and conclusions in section 5.

2. EXPERIMENTS

2.1. Equipment

A test loop including a pipe test section, a fluidization bed, surrounded by a "viewing box" of square cross-section, was set up. The column (figure 1) was constructed of a Duran 50 glass pipe with 63 mm i.d. and a length of 1000 mm. The test section was designed to permit visualization of the flow inside the fluidized bed and velocity measurements with an optical system (LDA). The fluidized bed consisted of 3.15 ± 0.1 mm dia Duran glass spheres, a small fraction of which was gold-coated. Brass gauzes at the upper and lower ends of the pipe were used in order to prevent stray particles from leaving the test section. The test liquid was a mixture of two diesel oils.

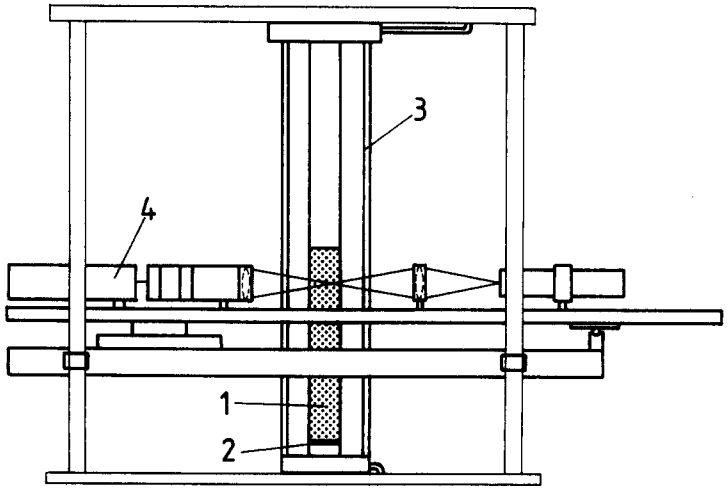

Figure 1. Test section: 1, fluidized bed; 2, lower gauze; 3, viewing box; 4, LDA system.

The motion of the coated particles in and above the fluidized bed was registered by a Hycam high-speed photographic camera, at 200–500 frame/s. The test section was illuminated by two quartz-halogen light sources (of 2000 W each) through an opalescent glass sheet.

The pictures taken by the high-speed camera were stationary projected on a screen. Because of refractive index matching the uncoated spheres were hardly visible on these pictures. The positions on the screen of selected coated particles were then marked by dark circles for successive frames of the high-speed camera. The resulting image of the particle motion was then photographed with a normal compact-film camera.

2.2. Results

The parameters of the experiment were as follows:

electric conductivity	$\sigma < 10^{-11}\ \Omega^{-1}/\text{cm}$,
fluid density	$\rho_f = 0.846\ \text{g/cm}^3$,
particle density	$\rho_p = 2.286\ \text{g/cm}^3$,
kinematic viscosity	$\nu = 4.53\ \text{mm}^2/\text{s}$,
volume flow rate	$\dot{V} \approx 12\ \text{l/min}$,
pipe diameter	$d = 63.5\ \text{mm}$.

The increase in diameter and weight of the glass particles due to the gold coating was neglected.

In order to produce the specific motion of the coated particles after a prolonged shutdown (e.g. overnight) of the test loop, a start-up time of about 30 min was necessary. After the establishment of a homogeneous fluidization, glass spheres were entrained, in areas of greater velocity, to a height of 1–2 cm above the bed surface. The uncoated spheres drifted back into the fluidized bed, whereas the coated ones continued to gather roughly 3 cm above the bed surface until about 50% of them accumulated in this region. Figure 2 is a photograph of such coated particles floating 30 mm above the bed surface.

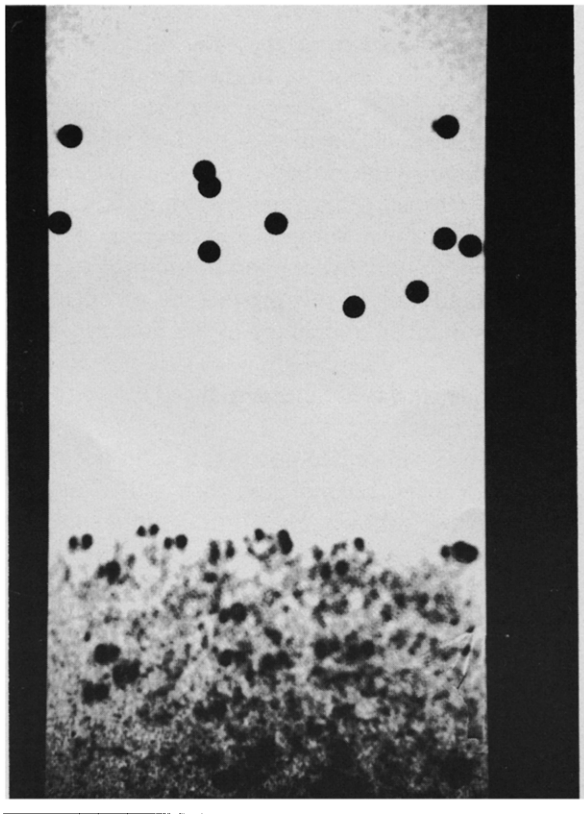

Figure 2. Floating layer of coated spheres above the fluidized bed.

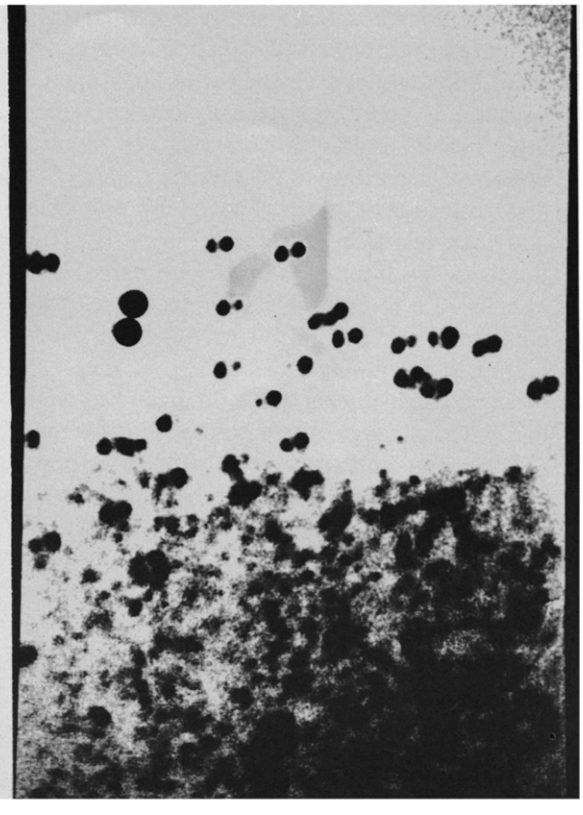

Figure 3. Collision of two conducting spheres.

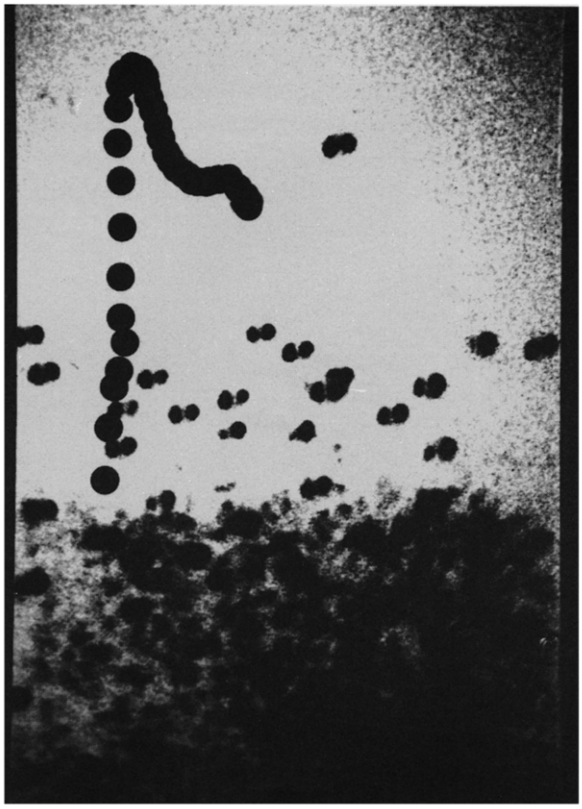

Figure 4. Rise of a sphere after collision.

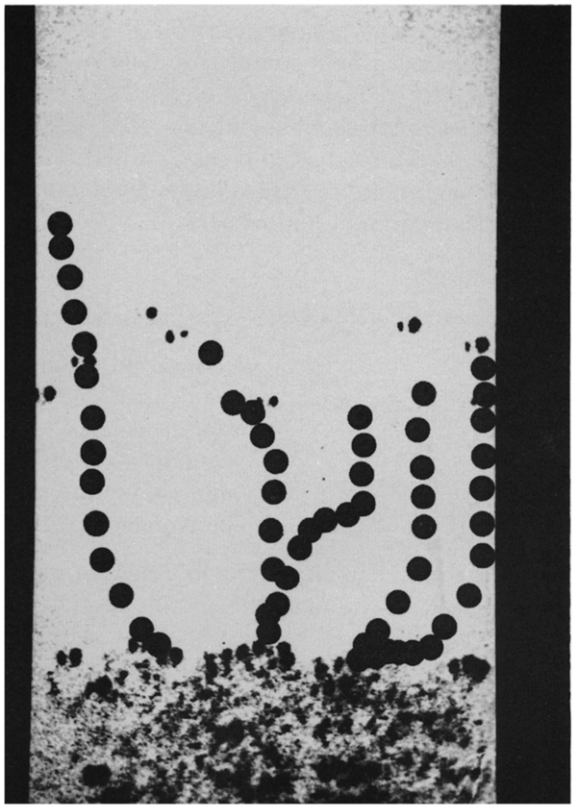

Figure 5. Settling of spheres after stopping the flow.

These coated spheres showed peculiar collision phenomena, which were not observed for the uncoated ones. When two such spheres approached the mentioned zone, they first attracted and then, upon contact, repelled with large axial and weak radial acceleration. In the case of an axial collision a sphere was typically carried at high speed to a height of 7–8 cm above the suspended layer before settling down slowly. In figure 3 the instant of collision of two marked spheres is visualized according to the procedure described above. In figure 4 the motion of two coated spheres after collision is shown. The sphere accelerated upwards reached a maximal height, sank a little and then rested in the floating layer. The sphere accelerated downwards in the direction of the fluidized bed interacted there with particles in the bed and was finally stopped in the bed, as can also be seen in figure 4. Different particles were subject randomly to this process. So an effective equilibrium existed in this exchange of particles and the number of spheres in the fluidized bed remained essentially constant.

The coated spheres in the fluidized bed collided in a similar fashion, but the induced motion was dissipated through interaction with other particles in the bed.

When the fluid stream was suddenly stopped, the fluidized bed settled down as a solid bed, but the coated spheres above the bed remained suspended for a few seconds and then settled in the middle of the bed surface. In figure 5 this sedimendation process is shown. The position of the spheres has not been marked here in constant time intervals, in order to make the form of the trajectory easier to recognize. The particle marked in the upper part of the figure started 450 pictures after the stop of the flow and the collapse of the fluidized bed to a fixed bed, i.e. 9 s after stopping (because of the recording velocity of 50 picture/s). The whole process shown in this figure lasted 23.4 s.

3. EQUATION OF PARTICLE MOTION AND FORCES

3.1. Equation of motion

The motion of the centre of mass $\mathbf{x}$ of a solid spherical particle of radius R (dia $D = 2R$) and density ρ_p in a Newtonian fluid of viscosity μ and density ρ_f ($\mu = \rho_f \nu$) is described, even at low

velocities, by a rather complicated equation (e.g. Maxey & Riley 1983; Parshikova 1983). This equation simplifies considerably if the flow of the fluid is assumed to be uniform and if the Basset history term is neglected:

$$m_p \frac{d^2\mathbf{x}}{dt^2} = \mathbf{F}_G + \mathbf{F}_I + \mathbf{F}_D + \mathbf{F}_E. \qquad [1]$$

In the range of low Reynolds numbers, where [1] has been derived, the forces have the expressions:

$$\left.\begin{aligned} \mathbf{F}_G &= (m_p - m_f)\mathbf{g} && \text{(gravity force)} \\ \mathbf{F}_I &= -\frac{1}{2} m_f \frac{d^2\mathbf{x}}{dt^2} && \text{(inertial force, added mass)} \\ \mathbf{F}_D &= -6\pi\mu R\left(\frac{d\mathbf{x}}{dt} - \mathbf{u}\right) && \text{(resistance force)} \\ \mathbf{F}_E &= \text{to be described} && \text{(electrostatic force).} \end{aligned}\right\} \qquad [2]$$

The significance of the parameters here is as follows: $m_p = (4/3)\pi\rho_p R^3$ is the particle mass; $m_f = (2/3)\pi\rho_f R^3$ is the added mass of the sphere; $\mathbf{g} = (0, 0, -g)$ is the vector of gravitational acceleration; and $\mathbf{u}$ is the fluid velocity at the site of the particle. The gravitational force $\mathbf{F}_G$ needs no further comment. The inertial force $\mathbf{F}_I$ is connected with the geometric form of the particle, since this influences the amount of fluid accelerated by its motion. For the drag force $\mathbf{F}_D$ at low particle Reynolds numbers,

$$\mathrm{Re} = \frac{D\left|\frac{d\mathbf{x}}{dt} - \mathbf{u}\right|}{\nu}, \qquad [3]$$

of about $\mathrm{Re} \leqslant 0.1$ (e.g. Batchelor 1983), the Stokes formula may be applied. For higher values of Re one has to introduce empirical expressions established for the drag force. At these values of Re, applying empirical formulae for the drag force in the equation of motion for a particle, one expects to get still at least qualitatively good results, of practical use.

Since in the situation considered in this paper one expects rather high Re, it is convenient to have an appropriate parametrization of the drag law over a wide range of Re. If one writes

$$\mathbf{F}_D = -3\pi\rho_f \nu D\left(\frac{d\mathbf{x}}{dt} - \mathbf{u}\right) C_D, \qquad [4]$$

with $C_D = 1$ for the Stokes force, then a satisfactory form of $\mathbf{F}_D$ for $\mathrm{Re} \leqslant 10^5$ is given by Brauer (1971):

$$C_D = 1 + \frac{1}{6}\mathrm{Re}^{1/2} + \frac{1}{60}\mathrm{Re}. \qquad [5]$$

The exact formula for the coefficient C_D is not important here, since it is not expected that the results will depend on the precise analytic form of the drag force.

There remains the other external force $\mathbf{F}_E$, which in the problem considered here is of an electric nature. For particle velocities of the order of several m/s one may safely consider the electric forces as being of electrostatic nature. The main observations described in the previous section can be explained essentially by the motion of an electrically conducting particle under the influence of another particle at rest of the same kind. Therefore, the introduction of the correct expression for the electric force is important and needs special consideration. As long as the diameters of the particles are negligible compared to their distance, their electrostatic interaction is that of pointlike charges and the force is the corresponding Coulomb force. For distances of the order of the particle diameter there appear, however, strong induction phenomena which cause a redistribution of the charges on the particle surfaces. The forces no longer depend exclusively on the values of the total charges but also on their distributions. In particular, the description of the collisions between such finite size particles needs a detailed analysis of the electric forces between conducting spheres of finite diameter.

3.2. Electostatic forces

The electrostatic energy U of two conducting spherical particles of radii R is determined by their charges Q_1 and Q_2, by the dielectric constant ϵ of the nonconducting medium wherein they are situated and by their (surface) distance z. For the situation sketched in figure 6, the electrostatic energy can be written as

$$U(z) = \frac{(Q_1+Q_2)^2}{4\epsilon}\frac{1}{C_{11}+C_{12}} + \frac{(Q_1-Q_2)^2}{4\epsilon}\frac{1}{C_{11}-C_{12}} \qquad [6]$$

in terms of two coefficients C_{11} and C_{12} which depend only on the distance z (and on the radius R, as a parameter). The derivation of [6] as well as the expression of these coefficients can be found, for example, in Buchholz (1957) or Kottler (1927). For the present considerations it will be enough to quote the corresponding results:

$$C_{11}(z) = R\sum_{n=1}^{\infty}\frac{\sinh\frac{1}{2}\alpha}{\sinh(n-\frac{1}{2})\alpha}, \qquad [7]$$

$$C_{12}(z) = -R\sum_{n=1}^{\infty}\frac{\sinh\frac{1}{2}\alpha}{\sinh n\alpha} \qquad [8]$$

and

$$\frac{\alpha}{2} = \ln\left\{1+\frac{z}{2R}+\left[\left(1+\frac{z}{2R}\right)^2-1\right]^{1/2}\right\},$$

$$\cosh\frac{\alpha}{2} = 1+\frac{z}{2R}. \qquad [9]$$

These series expansions converge for all values of $z > 0$; the rate of convergence deteriorates as one approaches smaller values of z and at $z = 0$ the series diverge.

At large distances, $z \to \infty$, the coefficients C_{11} and C_{12} behave like

$$C_{11} \approx R$$

and

$$C_{12} \approx -\frac{R^2}{z}.$$

Therefore, the electrostatic energy tends to

$$\lim_{z\to\infty} U(z) = \frac{1}{2\epsilon R}(Q_1^2+Q_2^2), \qquad [10]$$

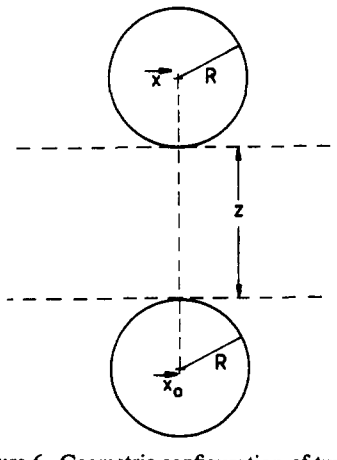

Figure 6. Geometric configuration of two identical (conducting) spheres.

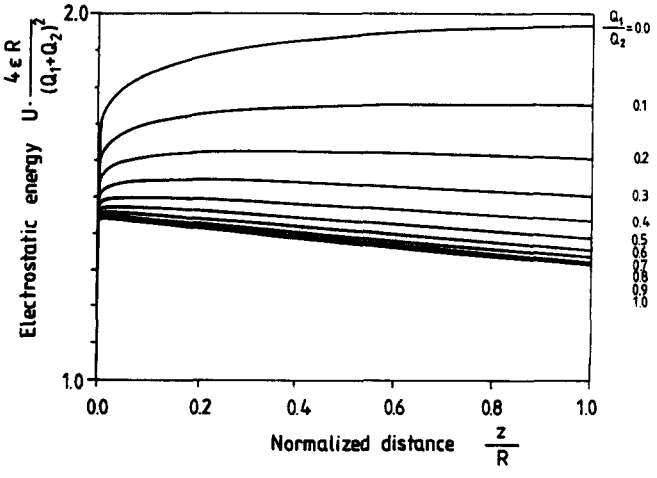

Figure 7. Normalized electrostatic energy $U(z)[4\epsilon R/(Q_1+Q_2)^2]$ of two conducting spheres of radius R, as a function of the distance z.

the sum of the individual energies of the two spheres. The behaviour of $U(z)$ (suitably normalized) is represented in figure 7.

As a consequence, one gets for $z \to \infty$ the behaviour of the electrostatic force $\mathbf{F}_E(z) = (0, 0, F_E(z))$,

$$F_E(z) = -\frac{dU(z)}{dz} \qquad [11]$$

acting on the upper sphere (having the centre coordinates $\mathbf{x} = (0, 0, z + R)$) in the configuration of figure 6 due to the presence of the lower sphere (of centre coordinates $\mathbf{x}_0 = (0, 0, -R)$):

$$F_E(z) = -2\frac{Q_1^2 + Q_2^2}{\epsilon R^2}\frac{R^5}{z^5} + \frac{Q_1 Q_2}{\epsilon z^2} + \cdots. \qquad [12]$$

This force depends essentially upon whether the quantity $Q_1 Q_2$ vanishes or not. If both charges are different from zero, the force is of Coulomb type for $z \to \infty$, $Q_1 Q_2/\epsilon z^2$. On the contrary, if $Q_1 Q_2 = 0$ because of say $Q_1 = 0$, then the force behaves like z^{-5}, being thus of short range. The force is attractive in this case and dependent on the third power of the particle radius (R^3). It represents the interaction between the charge $Q_1 \neq 0$ and the induced charge distribution (mainly a dipole) on the other sphere.

For the present investigations, the electrostatic force at small particle distances is of special interest. Since the series expansions [7] and [8] are not well-suited for the analysis of its behaviour, one has to use an asymptotic short distance expansion (e.g. Buchholz 1957):

$$C_{11} + C_{12} = \frac{1}{2}R \sinh\frac{\alpha}{2}\left[\frac{\ln 4}{\frac{\alpha}{2}} - \frac{1}{12}\frac{\alpha}{2} - \frac{7}{1440}\left(\frac{\alpha}{2}\right)^3 + O\left(\left(\frac{\alpha}{2}\right)^5\right)\right] \qquad [13a]$$

and

$$C_{12} = -\frac{1}{2}R \sinh\frac{\alpha}{2}\left[\frac{\left(C + \ln\frac{2}{\alpha}\right)}{\frac{\alpha}{2}} + \frac{1}{18}\frac{\alpha}{2} + \frac{7}{2700}\left(\frac{\alpha}{2}\right)^3 + O\left(\left(\frac{\alpha}{2}\right)^5\right)\right], \qquad [13b]$$

wherein $C = 0.57721566$ is the Euler constant. These expansions can be expressed by

$$\frac{\alpha}{2} = \left(\frac{z}{R}\right)^{1/2} + O\left(\left(\frac{z}{R}\right)^{3/2}\right)$$

in terms of z/R. They give

$$\lim_{z \to 0}(C_{11} + C_{12}) = R \ln 2 \qquad [14]$$

and, therefore,

$$\lim_{z \to 0} U(z) = \frac{(Q_1 + Q_2)^2}{4\epsilon R}\frac{1}{\ln 2}, \qquad [15]$$

which shows that the electrostatic energy of the spheres is, in the limit of contact, dependent only on their total charge $Q_1 + Q_2$. They also show that the behaviour of the force $F_E(z)$ near contact is essentially decided by $C_{11} - C_{12}$, i.e. by the second term in [6]. Otherwise stated, the behaviour of the force at small distances z depends on whether $Q_1 = Q_2$ or not. If the charges are equal ($Q_1 = Q_2 = Q$), then because of

$$\lim_{z \to 0}\frac{d}{dz}(C_{11} + C_{12}) = R\frac{1}{12}\left(\ln 4 - \frac{1}{2}\right) \qquad [16]$$

there will be a finite repulsive force at contact

$$\lim_{z \to 0} F_E(z) = \frac{Q^2}{\epsilon R^2}\frac{1}{(\ln 2)^2}\frac{1}{12}\left(\ln 4 - \frac{1}{2}\right). \qquad [17]$$

Since

$$\frac{1}{(\ln 2)^2}\frac{1}{3}\left(\ln 4 - \frac{1}{2}\right) = 0.6149,$$

this force is somewhat weaker than the Coulomb force at point charges ($Q_1 = Q_2 = Q$) located at a distance $2R$ from each other. If on the contrary $Q_1 \neq Q_2$, the force is decided for $z \to 0$ by $C_{11} - C_{12}$. Since

$$C_{11} - C_{12} \approx \frac{1}{2} R \ln \frac{R}{z} \qquad [18]$$

and

$$\frac{\mathrm{d}}{\mathrm{d}z}(C_{11} - C_{12}) \approx -\frac{1}{2}\frac{R}{z}, \qquad [19]$$

it is given by

$$F_E(z) \approx -\frac{(Q_1 - Q_2)^2}{2\epsilon R^2} \frac{1}{\frac{z}{R}\left(\ln \frac{z}{R}\right)^2}. \qquad [20]$$

The force is in this case attractive for small enough distances and even gets infinite at contact, with a singularity weaker than R/z (to be compared with the Coulomb singularity $1/z^2$).

These considerations concerning the behaviour of the electrostatic force $F_E(z)$ at large distances ($z \to \infty$) and near contact ($z \to 0$) already give a good qualitative background to the considerations in the introduction concerning the expected motion of charged conducting particles and the experimental observations given in section 2. They show that:

(a) At large distances ($z \to \infty$), there is an attractive force for charges $Q_1 Q_2 \leqslant 0$ and a repulsive (Coulomb) force for $Q_1 Q_2 > 0$. Thereby, the attractive force is Couloumb-like for nonvanishing charges ($Q_1 Q_2 < 0$) and of short range z^{-5} if one charge vanishes ($Q_1 Q_2 = 0$).
(b) At small distances ($z \to 0$), there is a finite force (essentially of Coulomb type) when the charges are equal ($Q_1 = Q_2$) and a singular attractive force otherwise ($Q_1 \neq Q_2$), of behaviour weaker than z^{-1}.

In the region in between nothing special is expected to happen as long as the charges have opposite sign ($Q_1 Q_2 < 0$): there is an attractive force changing from the behaviour $1/z^2$ at large distances to $1/Rz[\ln(z/R)]^2$ near contact. If one charge vanishes ($Q_1 Q_2 = 0$), an attractive force is expected, changing in its behaviour from $R^3 z^{-5}$ at $z \to \infty$ to $1/Rz[\ln(z/R)]^2$ at $z \to 0$. This is confirmed by numerical computation.

When the charges obey $Q_1 Q_2 > 0$, the estimates for large and small distances require the existence of a region of attraction at small distances and of one of repulsion at large distance, as long as the charges are not precisely equal. When $Q_1 = Q_2$, the estimates are compatible with a repulsive force between the spheres for all distances. This indeed happens. Figure 8 represents the connection between the charge ratio Q_1/Q_2 and the distance (z_e) where the regions of attraction and repulsion meet. The curve is the graphical representation of

$$F_E(z_e)\left(= -\frac{\mathrm{d}U}{\mathrm{d}z}\bigg|_{z=z_e}\right) = 0;$$

it shows that $z_e \to \infty$ for $Q_1/Q_2 \to 0$, and $z_e \to 0$ for $Q_1/Q_2 \to 1$, as suggested by the qualitative discussion.

It should be stressed again that the appearance of attractive forces between electric conductors at small distances, when carrying charges of the same sign, is an induction phenomenon which is essentially related to the finite extent of the conductors. It may be estimated that the distance range "z" of the appearance of these forces is roughly of the order of the size of the conductors.

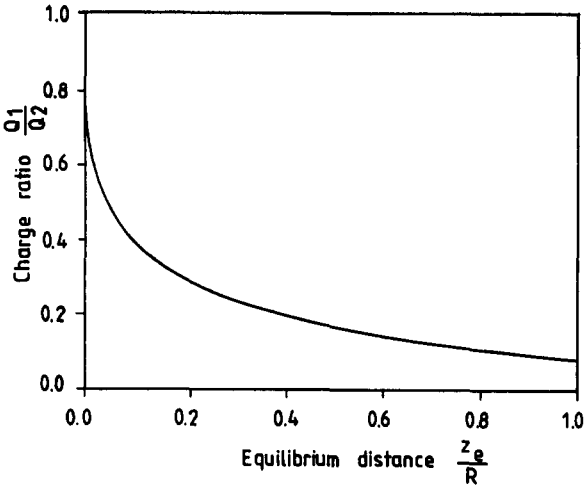

Figure 8. Relation between the equilibrium position z_e of two identical conducting spheres of radius R and their charge ratio Q_1/Q_2.

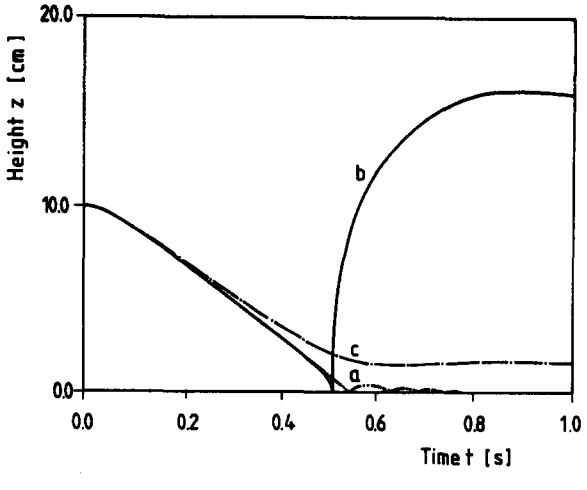

Figure 9. Evolution in time of the height z of the sphere under the influence of: (a) gravitation and realistic drag; (b) electric force between two conducting spheres added to (a), with $(Q_1+Q_2)/2 = 100$ e.s.u. and $Q_1/Q_2 = 0$ before collision; (c) same as (b), except that $Q_1/Q_2 = 0.005$. Initial data: $t_0 = 0$, $z_0 = 10$ cm, $\dot{z}_0 = 0$.

4. DESCRIPTION OF PARTICLE COLLISION

4.1. Qualitative description

In order to compare the description of particle motion in the fluid with observation one needs, in addition to the equation of motion [1], the parameters entering this equation and a reasonable knowledge of the initial conditions. The relevant parameters for the present considerations are the fluid velocity u and the charges Q_1 and Q_2. The experimental situation described implies a pipe flow (dia $d = 63.5$ mm) of rate around $\dot{V} = 12$ l/min, which corresponds to a mean fluid velocity $\bar{u} = 6.32$ cm/s and a (mean) Reynolds number $\mathrm{Re} = \bar{u}d/\nu = 8.85 \cdot 10^2$ well in the laminar range. The fluid velocity on the pipe axis is then $2\bar{u} = 12.64$ cm/s.

Before taking into account electric forces it will be adequate to develop an idea of the effects of the other forces, gravitation and friction, on the motion of particles. Assuming that the mobile sphere moves on (or close to) the pipe axis in the vertical direction and its motion starts at a height $z_0 \approx 10$ cm above the other sphere (at rest), with zero velocity, $\dot{z}_0 = 0$, as suggested by the experimental situation, one possesses all elements for the (qualitative) investigation of these forces. With gravity (and inertial force) alone, $\mathbf{g} = (0, 0, -g)$, [1] has, of course, an elementary solution, which gives a time t_G of "free" fall in the fluid, until the second sphere is reached, of

$$t_G = \left(\frac{2z_0}{g}\,\frac{\rho_p + \frac{1}{2}\rho_f}{\rho_p - \rho_f}\right)^{1/2}, \qquad z(t_G) = 0. \tag{21}$$

This time is, with the adopted data, $t_G = 0.1959$ s and the collision velocity $\dot{z}(t_G) = -102.09$ cm/s. Addition of the Stokes drag force still keeps the equation of particle motion elementary integrable.

The time t_S of "Stokes" fall will be (for $u = 10$ cm/s) $t_S = 0.2198$ s, and the collision velocity $\dot{z}(t_S) = -87.53$ cm/s.

At the moment of contact the particle Reynolds number would be about $\mathrm{Re} = 678$, which is far beyond the validity of the Stokes drag law. Therefore, an empirical drag law [4, 5], valid for a wide range of Reynolds numbers, has to be chosen. Thereby the equation of motion becomes nonlinear and has to be solved numerically. The stationary settling velocity is then determined from the equation

$$\mathrm{Re} + \frac{1}{6}\mathrm{Re}^{1/2} + \frac{1}{60}\mathrm{Re}^2 = \frac{1}{18}\left(\frac{\rho_p}{\rho_f} - 1\right)\frac{D^3 g}{\nu^2} \tag{22}$$

for the Reynolds number Re. Its solution for the data of the problem is 206.489 and gives a relative velocity

$$\dot{z}_\infty - u = -29.695 \text{ cm/s}, \tag{23}$$

i.e. a stationary settling velocity of

$$\dot{z}_\infty = -19.695 \text{ cm/s}. \quad [24]$$

This velocity is to be compared with $\dot{z}_G + u = -193$ cm/s, the settling velocity of the Stokes drag law. From this comparison one may infer that the "relaxation" time will be correspondingly smaller than that of the Stokes law,

$$\tau = \frac{m_p + \frac{1}{2}m_f}{6\pi\mu R} = \frac{1}{18}\frac{D^2}{\nu}\left(\frac{1}{2} + \frac{\rho_p}{\rho_f}\right) \quad [25]$$

($=0.39$ s). This, in turn, allows a reasonable estimate of the fall time t_D by considering that the particle falls from the beginning with the settling velocity

$$t_D \gtrsim -\frac{z}{\dot{z}_\infty} = 0.5077 \text{ s}. \quad [26]$$

Numerical computation shows that

$$t_D = 0.547 \text{ s} \quad [27]$$

and that the collision velocity is $\dot{z}(t_D) = -19.695$ cm/s, i.e. already the settling velocity. The settling velocity is, in fact, attained after about 1 cm of fall and a time of 0.1 s. This implies that, if the initial position z_0 of the sphere were lowered to 1 cm, the drag and gravity forces would not change the picture of motion, leaving, for example, the collision velocity, and thereby the whole later development of motion, unaltered.

As far as the nature of the collision of the falling particle with another at rest is concerned, it is not unreasonable to assume that it is elastic, i.e. the kinetic energy does not decrease and that the recoil is taken over by the support of the fixed sphere. Then, the velocity of the falling sphere will only change sign by the collision at $z = 0$ and keep its magnitude.

Electric forces may, of course, change the described picture, as will be seen in the following.

It is appropriate to ask how a particle arrives at the height z_0, which was taken as initial position in the investigation of its motion. The mechanism has to have connection with the electric charges the particles bear, although it can not be traced precisely. It can, however, lead to the question about the order of magnitude of the electric charge necessary to keep one sphere above the other at rest against gravity and drag force at a height of about z_0. In order to estimate it, it is enough to consider for the electric force the Coulomb law. For equal charges $Q_1 = Q_2 (= Q)$ one gets hereby

$$Q = (-F_G - F_D)^{1/2}\sqrt{\epsilon}(z_0 + D), \quad [28]$$

with $z_0 = 10$ cm about $Q = 66$ e.s.u.

If one now develops the scenario that a particle falls, with a charge of say $Q_1 = 140$ e.s.u. from the initial position of about $z_0 = 10$ cm with zero velocity $\dot{z}_0 = 0$, down towards a second particle of zero charge $Q_2 = 0$, then in the absence of the Coulomb force ($Q_1 Q_2 = 0$) the motion has to be dominated by gravity and drag forces to distances where the induction forces start to get significant. When these forces are felt, the sphere should be accelerated, at very small distances very strongly, since the attractive force gets (singularly) large. The velocity should thereby stay, however, finite, since the singularity of the force is integrable.

There remains now to be investigated qualitatively the motion when both charges are different from zero. In the present experiments it is not to be expected that $Q_1 Q_2 < 0$, but even if this happens, the only effect will be an additional acceleration of the falling. If $Q_1 Q_2 > 0$, the falling will be accelerated at first if z_0 lies above the equilibrium position:

$$\frac{(Q_1 Q_2)^{1/2}}{\sqrt{\epsilon}}(-F_G - F_D)^{1/2} - D. \quad [29]$$

Then it will be decelerated until the height z of transition from repulsive to attractive force is reached (if at all!), below which again acceleration takes place. If in the deceleration region the particle reaches zero velocity, it will return upwards and in the long run it will achieve an oscillatory behaviour around the equilibrium position [29].

As an illustration, take $\frac{1}{2}(Q_1 + Q_2) = 100$ e.s.u., $Q_2/Q_1 = 0.005$, which means $Q_1 Q_2 = 198$ e.s.u.^{2}. Then the approximate equilibrium position will be $z = 1.878$ cm, or $z/R = 11.924$. For the charge

ratio $Q_2/Q_1 = 0.005$ the transition point from repulsion to attraction lies at $z/R = 5.435$, below the expected equilibrium position. For these data one thus expects the approach to equilibrium without collision.

In the following, quantitative computations will be presented.

4.2. Quantitative description

The equation of motion [1] has been solved numerically, with the forces $\mathbf{F}_G$ and $\mathbf{F}_I$ given by [2], the drag force $\mathbf{F}_D$ by [4] and [5] and the electric force $\mathbf{F}_E$ by [11]. The physical constants have been chosen according to the experimental situation described in section 2 and the total electric charge $Q_1 + Q_2$ has been varied in the range $100\,\text{e.s.u.} \leqslant Q_1 + Q_2 \leqslant 200\,\text{e.s.u.}$ The time interval of investigation is determined by the fall with the realistic drag law and an initial height of about $z_0 = 10\,\text{cm}$; the collision phenomena of interest will take place within 1 s. The algorithm of solution is a (standard) Runge–Kutta method of fourth order. The only problem in computation to mention is, that the equation gets singular at $z = 0$ because of the divergence of the electric force. But it is rather harmless, because the velocity is not infinite at $z = 0$, although the acceleration (force) is, and for small positive values there is the asymptotic expansion, due to [13], of the electric force, which one can use instead of the badly convergent series expansions [7] and [8]. So in the last step of computation before collision one has only to take care not to have to compute the force precisely at $z = 0$. One can get rather good quantitative estimates of the velocity $\dot{z}_c$ near $z = 0$ by considering appropriately the energy theorem. An example of such an estimate, with $(Q_1 + Q_2)/2 = 10^2$ e.s.u., is

$$-848\,\text{cm/s} < \dot{z}_c < -826\,\text{cm/s}, \qquad [30]$$

with a precision of about 2.5%. In principle, an arbitrarily precise value of the collision velocity may be achieved. Practically, however, the computations are performed close to $z = 0$ and the last computed velocity is identified with $\dot{z}_c$, the collision velocity. Thereby the collision velocity is underestimated. For the trajectory after collision, this underestimate plus the hypothesis of elastic reflection (incident velocity = emergent velocity) amounts to the fact that in reality the emergent velocity (as computed) is smaller than the real incident velocity: the (computational) underestimate of the incident velocity amounts to a degree of inelasticity in the particle collision. Therefore, even if there is a velocity underestimate of about 10%, this amounts to a collision with about 20% of loss in kinetic energy, which is a physically entirely realistic result.

The computing algorithm has been checked first without the (singular) electrostatic force. The computation with gravity and realistic drag force shows that stationary settling is indeed achieved after a distance of about 1 cm. In figure 9 this motion is represented for the purpose of comparison. Also given are two other trajectories determined by electrostatic forces. One trajectory starts at $z_0 = 10\,\text{cm}$ with $\dot{z}_0 = 0$ (at $t = 0$) in the situation where only one particle is electrically charged: $Q_1 = 0$, $Q_2 = 200$ e.s.u. before collision.

One notices that down to small distances (about 2 cm) the (short-range) electric force is not felt; the trajectory coincides with that given in the absence of an electric force. Then one sees the increasing (attraction and) acceleration. At $z = 0$ the charge redistribution takes place to $Q_1' = Q_2' = 100$ e.s.u. (assumed to be instantaneous) and the following steep rise is the consequence of the strong repulsive Coulomb force. An underestimate of the recoil velocity, i.e. an inelastic collision leads only to a very small change in the rise of the particle after collision. It turns out that the rising to equilibrium is highly insensitive to the recoil velocity $\dot{z}$ at $z = 0$.

Again, for the purpose of distinguishing between short- and long-range forces during the downwards motion before collision, the trajectory with charges of about $Q_1 = 1$ e.s.u. and $Q_2 = 199$ e.s.u. ($Q_1 + Q_2 = 200$, $Q_1/Q_2 = 0.005$) is shown in figure 9. The (long-range) Coulomb force is perceived on practically the whole trajectory of the particle and prevents the approach of the two spheres to contact.

5. CONCLUSIONS AND COMMENTS

A particular kind of collision phenomenon of electrically conducting particles in a nonconducting fluid, above a fluidized bed, has been investigated in the present paper. In the experiment performed

a strong acceleration of two such spheres towards each other before the collision has been observed, followed by a strong acceleration away from each other after the collision. This behaviour cannot be explained by hydrodynamic forces, viscous or inertial. Although the motion before collision has some similarity with what Fortes *et al.* (1987) describe as drafting and kissing, an inertial effect associated with wakes, the tremendous acceleration observed after collision differs entirely from their tumbling phenomenon. It can however be explained, even rather quantitatively, in a natural way by the specific character which the electrostatic force between conducting spheres takes at distances of the order of their diameter: as a consequence of induction this force becomes attractive, even if the spheres carry (total) charges Q_1 and Q_2 of the same sign, provided $Q_1 \neq Q_2$.

Because of the fact that the phenomenon is dominated by electrostatic forces, it is not necessary to insist in its description on the precise equation of motion of the particles in the fluid, unless a high precision comparison between experiment and theory is considered. Such a comparison would then have to take, of course, into account finite particle distance corrections to viscous and inertial forces of the fluid, at lower Reynolds numbers, and to face the difficult question about the meaning and precise form of the equations of motion of particles at high Reynolds numbers.

Acknowledgements—This work has been supported in part by the "Deutsche Forschungsgemeinschaft" within "Teilprojekt A4" of the "Sonderforschungsbereich 222" of the University Erlangen-Nürnberg. The completion of the manuscript was aided by Mr F. Kaschak.

REFERENCES

BATCHELOR, G. K. 1983 *An Introduction to Fluid Dynamics*. Cambridge Univ. Press, Cambs.

BRAUER, H. 1971 *Grundlagen der Ein- und Mehrphasenströmungen*. Sauerlander, Aarau.

BUCHHOLZ, H. 1957 *Elektrische und magnetische Potentialfelder*. Springer, Berlin.

FORTES, A. F., JOSEPH, D. D. & LUNDGREN, T. S. 1987 Nonlinear mechanics of fluidization of beds of spherical particles. *J. Fluid Mech.* **177**, 467–483.

KOTTLER, F. 1927 *Elektrostatik der Leiter, Handbuch der Physik*, Vol. 12 (Edited by GEIGER, H. & SCHEEL, K.). Springer, Berlin.

MAXEY, M. M. & RILEY, J. J. 1983 Equation of motion for a small rigid sphere in a nonuniform flow. *Phys. Fluids* **26**, 883–889.

PARSHIKOVA, N. V. 1983 Spherical particles in an inhomogenous nonstationary flow. *Moscow Univ. mech. Bull.* **36**, 68–71.